

The effects of chemical reaction, Hall and ion-slip currents on MHD flow with variable thermal conductivity

S. S. Mustafa *, Rasha A. Mohamed

Department of Physics, Faculty of Education, Ain Shams University,
Roxy, Heliopolis, Cairo, Egypt

Abstract

In this paper, the problem of heat and mass transfer to the magneto-hydrodynamic (MHD) flow of a micropolar, viscous, incompressible, and electrically conducting fluid with suction and blowing through a porous medium under the effects of chemical reaction, Hall, ion-slip currents, and variable thermal conductivity is studied numerically by using finite difference method. The governing fundamental equations on the assumption of a small magnetic Reynolds number are approximated by a system of nonlinear ordinary differential equation. Details of the velocities, temperature and concentration fields are presented for the various values of the parameters of the problem, e.g., magnetic, chemical reaction, Hall, ion-slip, porous, thermal conductivity and surface mass transfer parameters. The numerical results indicate that the concentration decreases as the ion-slip, Hall parameters increase. Also, it decreases as the chemical reaction, Schmidt number increase.

Key words: chemical reaction – Hall and ion – slip - MHD

Nomenclature

f	Dimensionless stream function	x	Distance along the surface
f_w	Porosity parameter	y	Distance normal to the surface
h	Dimensionless microrotation	c	Species concentration in the fluid
G	Microrotation parameter	c_∞	Species concentration with fluid away from the plate
G_1	Microrotation constant	c_w	Species concentration near the plate
N_1	Coupling constant parameter	D	Chemical molecular diffusivity
κ	Chemical reaction parameter	Sc	Schmidt number
K	Coupling constant	n	Rate of chemical reaction
Re	Reynolds number	M	The magnetic constant
N	Microrotation component	ψ	Stream function
u	Velocity in the x-direction	φ	Dimensionless concentration function
U_o	Uniform velocity of the plate	γ	Non-dimensional chemical reaction parameter
U_∞	Velocity in the ambient fluid	η	Similarity variable
v	Velocity in the y-direction	μ	The dynamic viscosity
ρ	Density of the fluid	σ	Magnetic permeability
V_w	Wall suction/injection velocity	B_o	Magnetic induction
τ	The shear stress	B	Magnetic field
J	Current density	E	Electric field
k_f	The fluid thermal conductivity	p	pressure
k_∞	The fluid free stream thermal conductivity	T	The fluid temperature
s	The thermal conductivity parameter	T_∞	The fluid free stream temperature
w	Velocity component in z-axis	T_w	The plate temperature of the fluid
ω	Collision frequency	U_s	Surface velocity

* Corresponding author Email: s.s.shaban@edu.asu.edu.eg & dr.samia1960@yahoo.com

ν_e	Electron-atom collision frequency	c_p	Specific heat at constant pressure
n_e	Number density of electrons	β_e	Hall parameter
e	The charge on an electrons	β_i	Ion-slip parameter
$1/en_e$	Hall current factor	A, b	constants
J_x	Current density in x-axis	g	Dimensionless angular velocity function
J_z	Current density in z-axis	θ	Dimensionless temperature function
ν	The kinematics viscosity	K_p	Permeability parameter
Nu	Nusselt number	τ_w	Shear stress in x-axis
q_w	The local heat flux	τ_z	Shear stress in z-axis
Sh	Sherwood number	k^*	Porous medium constant

1. Introduction

The classical Navier-Stokes theory does not describe the flow properties of polymeric fluids, colloidal suspension and fluids containing certain additives. Eringen [1] proposed the theory of micropolar fluids, which show microrotation effects as well as microinertia. The theory of thermo micro polar fluids was developed by Eringen [2] by extending his theory of micropolar fluids. The theory of micropolar fluids is generating a lot of interest and many classical flows are being re-examined to determine the effects of fluid microstructure. It may form suitable non-Newtonian fluid models that can be used to explain the flow of colloidal fluids, liquid crystals, polymeric suspension, animal blood, and etc [3].

Several engineering situations arise in which mass is transferred through a fluid including condensation, sublimation and evaporation on a plate or on the inner surface of a tube. In some cases the surface reacts with the fluid. The reaction rate is both influenced by the kinetic laws, which governs the chemical reaction, and the transport mechanisms induced by hydromagnetic equations. The study of chemical reaction with heat transfer in porous medium has important engineering applications e.g. tubular reactors, oxidation of solid materials and synthesis of ceramic materials. Studies have been done under different physical conditions by Malashetty et al [4], El Tawil and Hassanein [5].

In general the study of magneto hydrodynamic flow behavior of viscoelastic fluid taking into consideration the porosity effects, heat and mass transfer with chemical reaction, Hall and ion slip current, have aroused the interest of many investigators [6], [7], [8], [9], [10], [11], [12].

The purpose of the present investigations is to study numerically the mass transfer characteristics of a steady, incompressible, magneto-micropolar fluid flowing past an isothermal plate with suction and blowing through a porous medium under the effects of chemical reaction, Hall, ion-slip currents, and variable thermal conductivity by using finite difference method.

This subject has important engineering applications such as geothermal systems, crude oil extraction and ground-water pollution.

2. Mathematical Formulation

A steady, incompressible, magneto-micropolar, and electrically conducting fluid flowing past a horizontal plate in the x-direction under the effects of mass transfer with chemical reaction is considered, variable thermal conductivity through a porous medium. The flow is subjected to a strong transverse magnetic field with a constant intensity along the y-axis. We assume that the induced magnetic field is neglected. In general, for an electrically conducting fluid, Hall and ion-slip currents affect the flow in the presence of a strong magnetic field. The effect of Hall current gives rise to force in the z-direction, which induces a cross flow in that direction and hence the flow becomes three-dimensional. To simplify the problem, we assume that there is no variation of flow or heat and mass transfer quantities in z-direction. The generalized Ohm law including Hall currents is

$$J = \frac{\sigma}{1 + \left(\frac{\omega}{\nu_e}\right)^2} \left(E + V \times B - \frac{1}{en_e} J \times B \right)$$

given in the form [13].

Where σ is the electrical conductivity, J is the electric current vector, V is the velocity vector, E is the intensity vector of the electric field, B is the magnetic induction vector, $(1/ene)$ is the Hall factor, (ω/ν_e) is the Hall parameter, n_e is the number density of the electrons, e is the charge on an electron, ν_e is the electron-atom collision frequency, and ω exceeds the collision frequency. When the ratio (ω/ν_e) becomes very large, the electromagnetic field can force both the ions and the electrons to produce a relative drift between them and neutral particles. This drift is called "ion-slip" and is of course negligible for highly ionized gases. It assume

$$k_f = k_\infty (1 + s\theta)$$

that $E = 0$ and the fluid properties are isotropic and constant except for the fluid thermal conductivity, which is

$$s = a(T_w - T_\infty)$$

assumed to vary as a linear function of temperature the form [13].

$$k_f = k_\infty (1 + a(T - T_\infty))$$

This form can be rewritten as following

Where

The velocity component u on a sheet is proportional to its distance from the slit. Then the governing equation within the boundary layer approximation may be written as follow [13].

$$u \frac{\partial u}{\partial x} + v \frac{\partial v}{\partial y} = 0 \tag{1}$$

$$u \frac{\partial u}{\partial x} + v \frac{\partial u}{\partial y} = \nu \frac{\partial^2 u}{\partial y^2} + \frac{K}{\rho} \frac{\partial N}{\partial y} - \frac{B_o}{\rho} J_z - \frac{\mu}{\rho k^*} u \tag{2}$$

$$u \frac{\partial w}{\partial x} + v \frac{\partial w}{\partial y} = \nu \frac{\partial^2 w}{\partial y^2} + \frac{B_o}{\rho} J_x - \frac{\mu}{\rho k^*} w \tag{3}$$

$$G_1 \frac{\partial^2 N}{\partial y^2} - 2N - \frac{\partial u}{\partial y} = 0 \tag{4}$$

$$u \frac{\partial T}{\partial x} + v \frac{\partial T}{\partial y} = \frac{1}{\rho c_p} \frac{\partial}{\partial y} \left(k_f \frac{\partial T}{\partial y} \right) + \frac{\nu}{c_p} \left(\frac{\partial u}{\partial y} \right)^2 \tag{5}$$

$$u \frac{\partial c}{\partial x} + v \frac{\partial c}{\partial y} = D \frac{\partial^2 c}{\partial y^2} - \kappa c \tag{6}$$

The generalized Ohms law including Hall and ion-slip

Where $\sigma_e = 1 + i\sigma_e$, subject to the boundary conditions

$$u = U_s = bx, v = -V_w, w = 0, N = 0, T = T_w, c = c_w, \text{ at } y = 0$$

$$u \rightarrow \infty, w \rightarrow 0, N \rightarrow 0, T \rightarrow T_\infty, c \rightarrow c_\infty, y \rightarrow \infty$$

By using the following similarity transformations

$$\eta = \sqrt{\frac{b}{\nu}} y \quad \theta(\eta) = \frac{T - T_\infty}{T_w - T_\infty} \quad \varphi(\eta) = \frac{c - c_\infty}{c_w - c_\infty} \quad N = \sqrt{\frac{b^3}{\nu}} x h(\eta) \quad (7)$$

$$u = bx f'(\eta) \quad v = -\sqrt{b\nu} f(\eta) \quad w = \sqrt{b\nu} x g(\eta) \quad (8)$$

Substituting (8) into (1)-(7) produces the following similarity equations and boundary conditions

$$f''(\eta) + f(\eta)f'(\eta) - (f'(\eta))^2 + N_1 h'(\eta) + \frac{M}{\alpha_e^2 + \beta_e^2} (\alpha_e f(\eta) + \beta_e g(\eta)) - \frac{1}{k_p} f(\eta) = 0 \quad (9)$$

$$g''(\eta) - f(\eta)g(\eta) + g'(\eta)f(\eta) - \frac{M}{\alpha_e^2 + \beta_e^2} (\alpha_e g(\eta) - \beta_e f(\eta)) - \frac{1}{k_p} g(\eta) = 0 \quad (10)$$

$$Gh'(\eta) - 2h(\eta) - f'(\eta) = 0 \quad (11)$$

$$\theta''(\eta) + \left(\frac{s}{1 + s\theta(\eta)}\right)(\theta'(\eta))^2 + \left(\frac{Pr}{1 + s\theta(\eta)}\right)(f(\eta)\theta'(\eta) + Ec(f'(\eta))^2) = 0 \quad (12)$$

$$\varphi''(\eta) + Scf\varphi'(\eta) - Sc\gamma Re\varphi(\eta) = 0 \quad (13)$$

$$F(0) = f_w, f'(0) = 1, g(0) = 0, h(0) = 0, \theta(0) = 1, \varphi(0) = 1 \quad (14)$$

Where

The coupling constant parameter $N_1 = K / (\rho\nu)$,

The microrotation parameter $= (G_1 b) / (\nu)$,

The Prandtl number $Pr = (\rho\nu c_p) / (k_\infty)$,

The Eckert number $Ec = U_s^2 / [c_p (T_w - T_\infty)]$,

The permeability parameter $k_p = (\rho k^* b) / (\mu)$,

The magnetic parameter $M = (\sigma B_\infty^2) / (b\rho)$,

$$f(\infty) = 0, g(\infty) = 0, h(\infty) = 0, \theta(\infty) = 0, \varphi(\infty) = 0$$

The Schmidt number $Sc = \nu/D$,

The chemical reaction parameter $\gamma = (\kappa\nu)/U_s^2$,

And the mass transfer parameter $f_w = V_w / (\sqrt{b\nu})$, which is positive for suction and negative for injection.

The physical quantities of interest in this problem are the following [11]

$$\tau_w = ((\mu + K) \frac{\partial u}{\partial y} + K(N))_{y=0}$$

$$\tau_w = ((\mu + K)bx \sqrt{\frac{b}{v}} f'(0))$$

By using (8)

Similarly

$$\tau_z = (\mu + K) \left(\frac{\partial w}{\partial y} \right)_{y=0} = (\mu + K)bxg'(0)$$

$$q_w(x) = -k_f \left(\frac{\partial T}{\partial y} \right)_{y=0} = -k_f (T_w - T_\infty) \sqrt{\frac{b}{v}} \theta'(0)$$

$$h(x) = \frac{q_w(x)}{(T_w - T_\infty)} = -k_f \sqrt{\frac{b}{v}} \theta'(0)$$

$$Nu_x = \frac{h(x)}{k_f} = -\sqrt{\frac{b}{v}} \theta'(0)$$

Where τ_w , and τ_z are the shear stress at the wall. The local heat flux may be written as follows

The local heat transfer coefficient is given by

The local Nusselt number may be written as

And the mass transfer coefficient in terms of the Sherwood number is given in the following form [11]

$$Sh = \frac{-x}{c_w} \left(\frac{\partial c}{\partial y} \right)_{y=0} = \frac{-x}{c_w} (c_w - c_\infty) \sqrt{\frac{b}{v}} \phi'(0)$$

3. Numerical Solution

The set of ordinary differential equations (9) – (13) with boundary condition (14) have been solved using finite difference method with $Sc, fw, \gamma, N1, Pr, Ec, kp, M, s, G$ as prescribed parameters.

A program using symbolic and computational computer language (Mathematica 4.0) did the computations.

4. Results and discussion

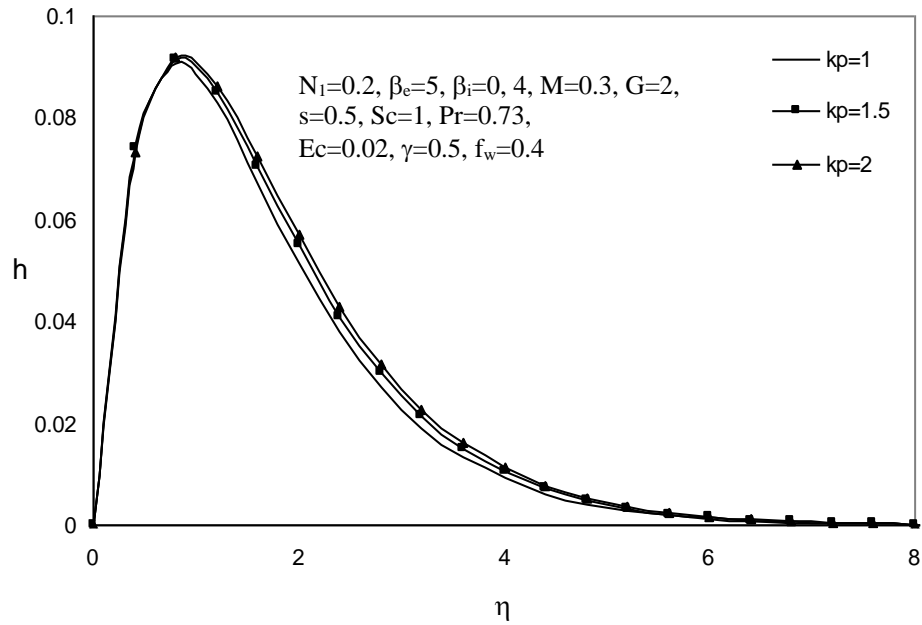


Fig. 1 Microrotation profiles for various values of porous medium parameter

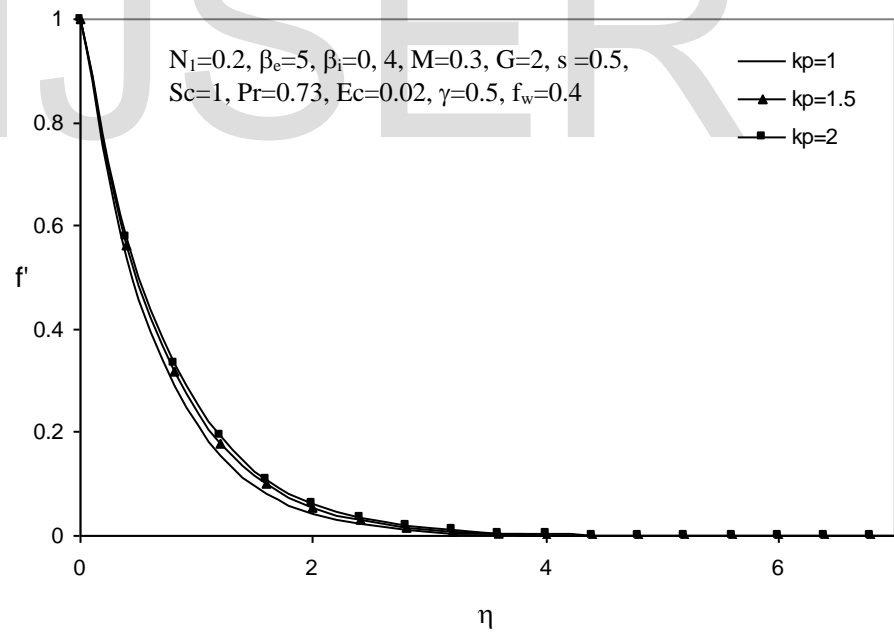


Fig.2 Velocity profiles for various values of porous medium parameter

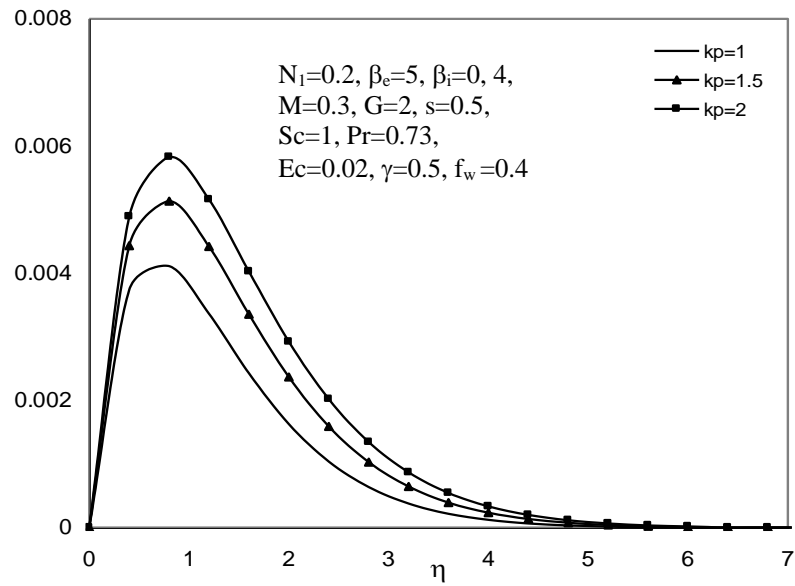


Fig.3 Angular velocity profiles for various values of porous medium parameter

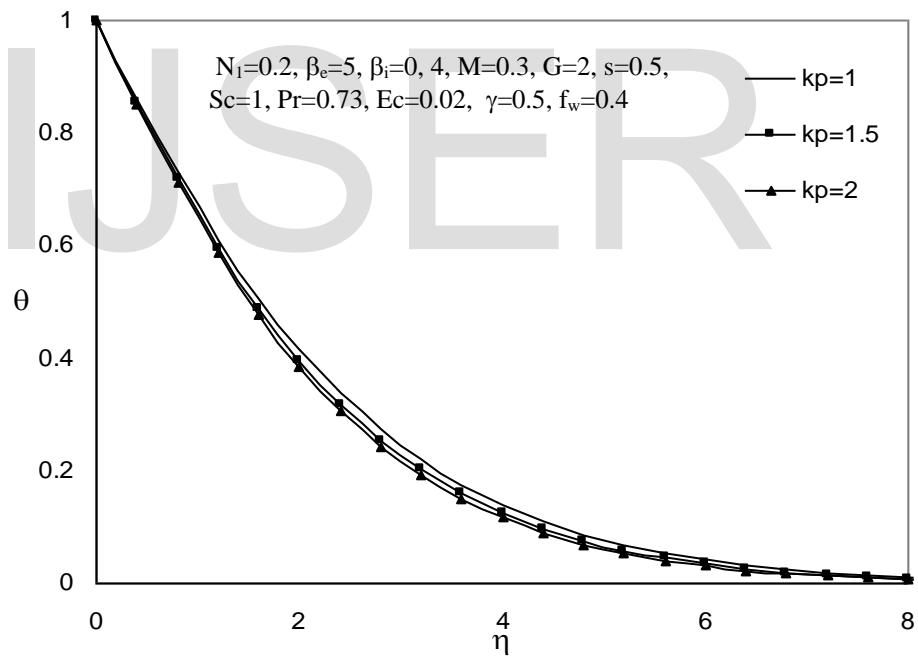


Fig.4 Temperature profiles for various values of porous medium parameter

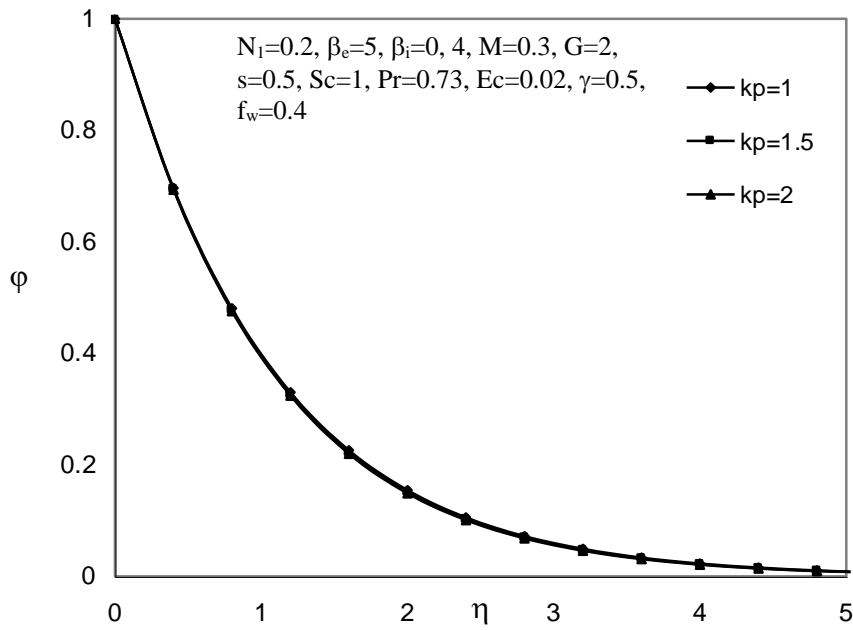


Fig.5 Concentration profiles for various values of porous medium parameter

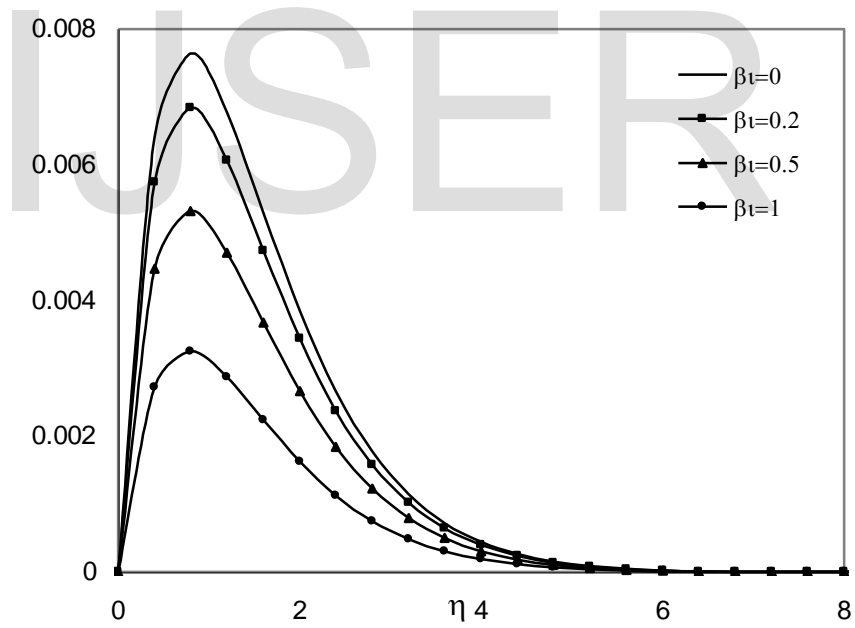


Fig.6 Angular velocity profiles for various values of ion-slip parameter

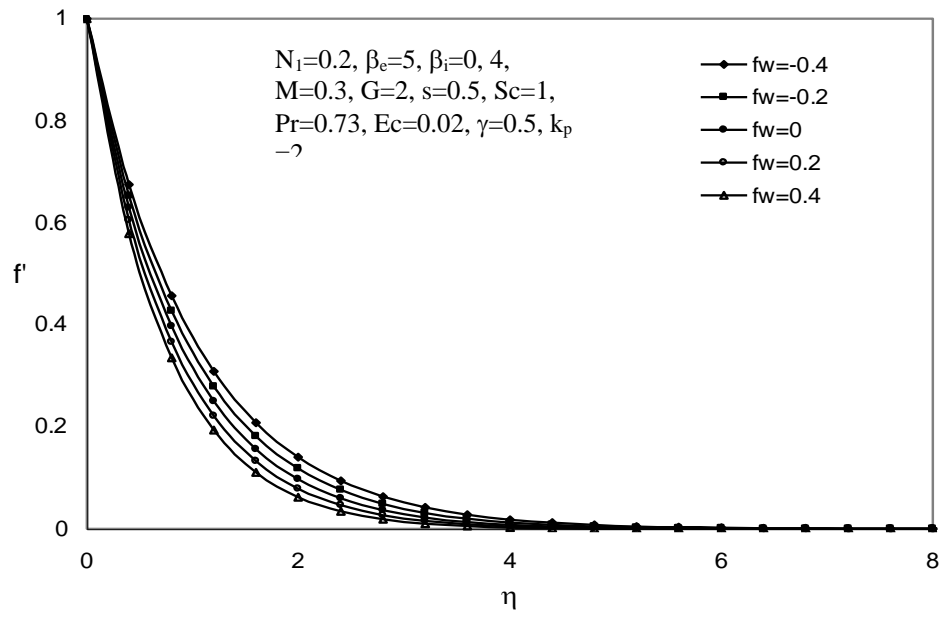


Fig.7 Velocity profiles for various values of mass transfer parameter

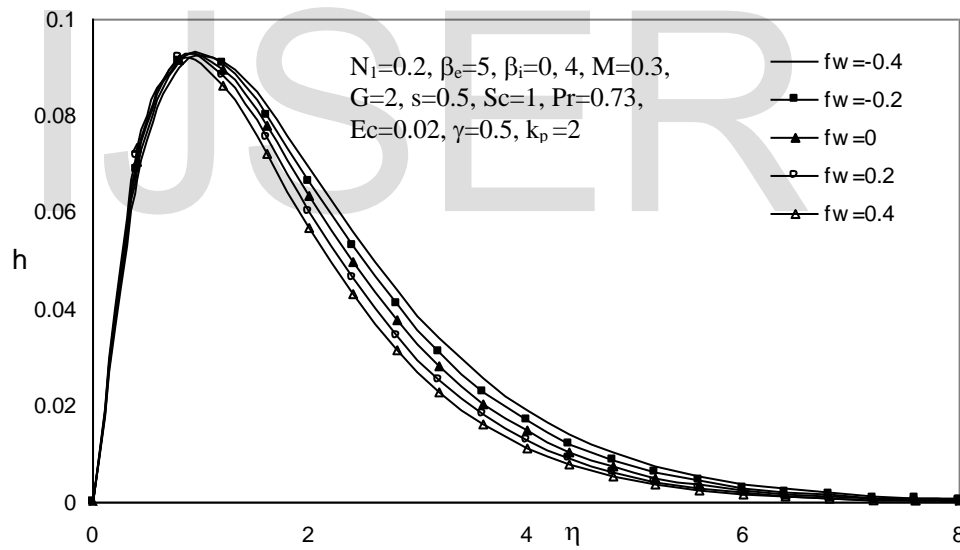


Fig.8 Microrotation profiles for various values of mass transfer parameter

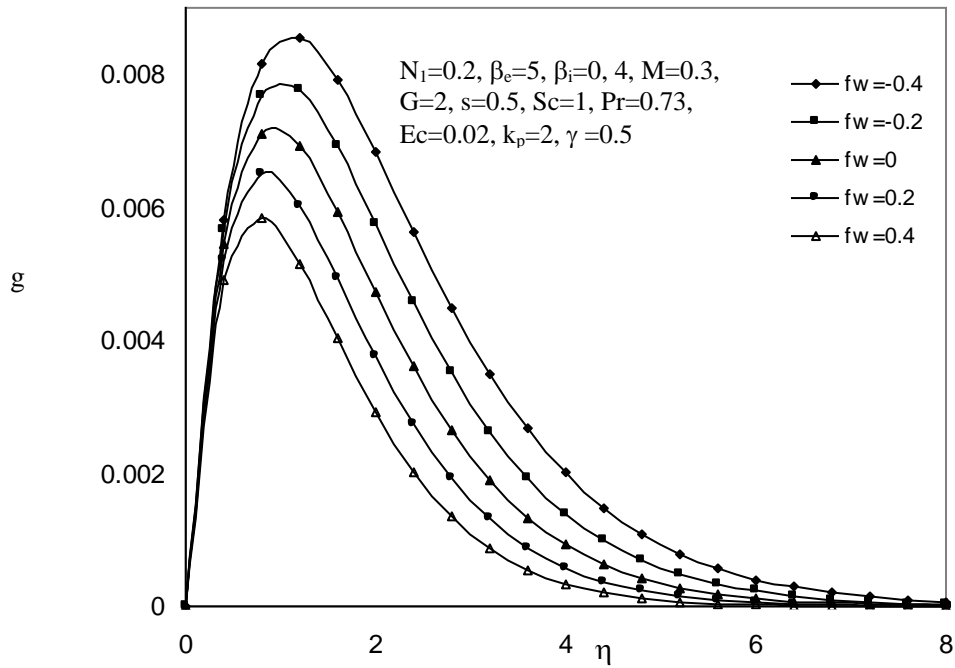


Fig.9 Angular velocity profiles for various values of mass transfer parameter

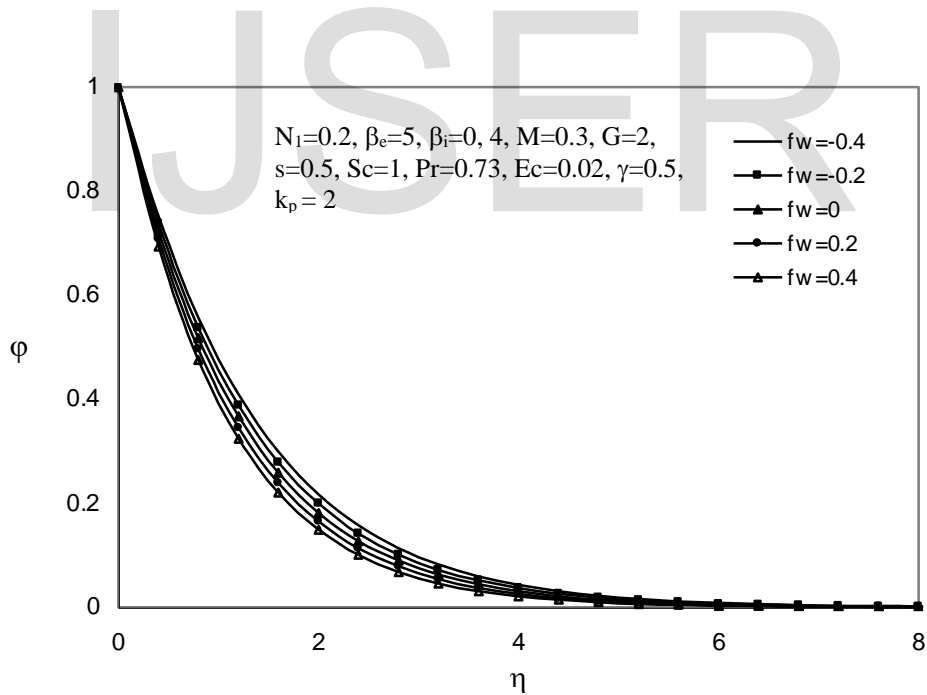


Fig.10 Concentration profiles for various values of mass transfer parameter

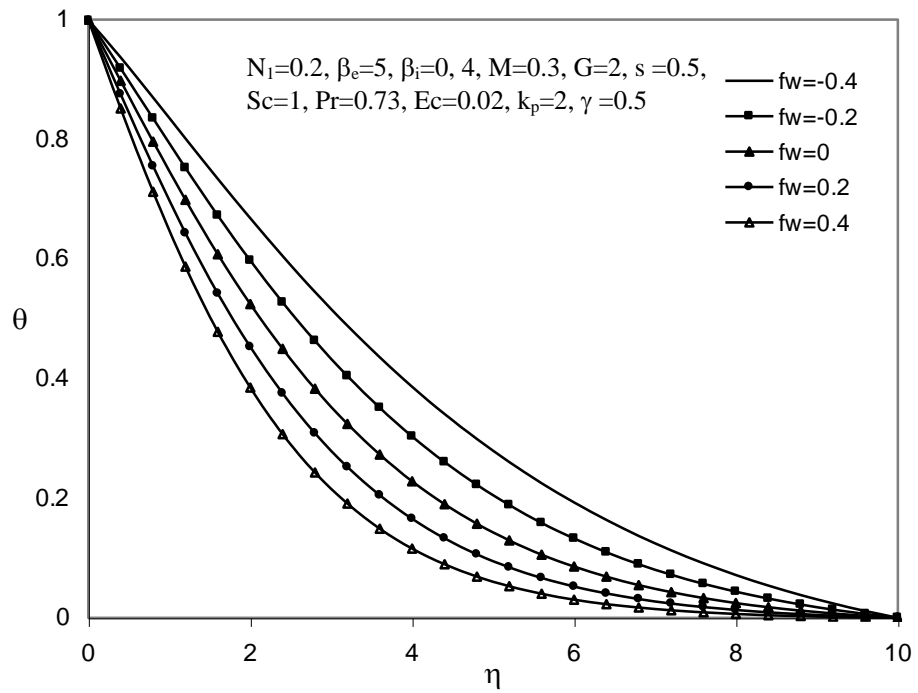


Fig.11 Temperature profiles for various values of mass transfer parameter

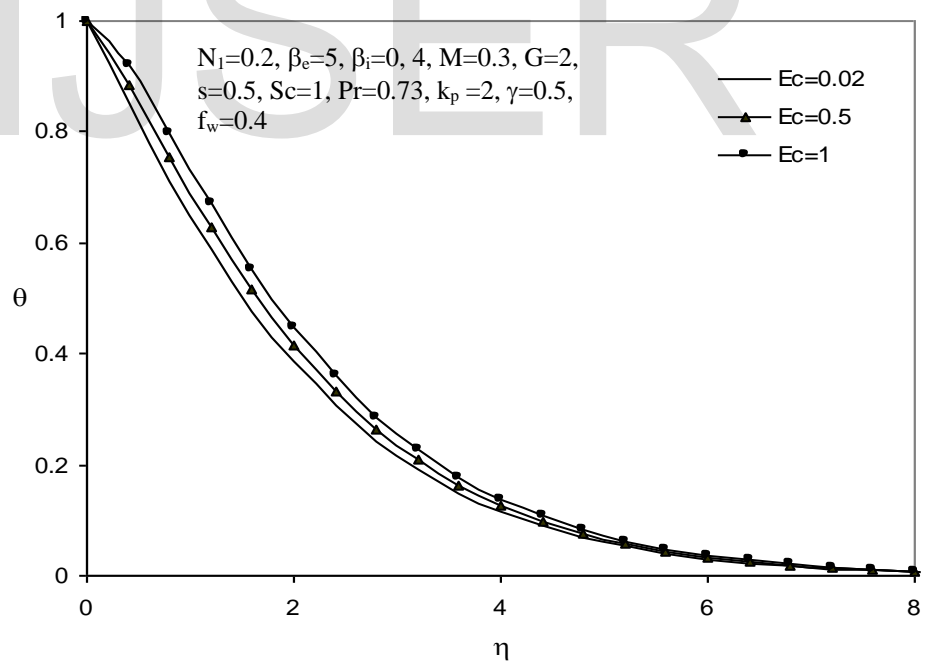


Fig.12 Temperature profiles for various values of Eckert number

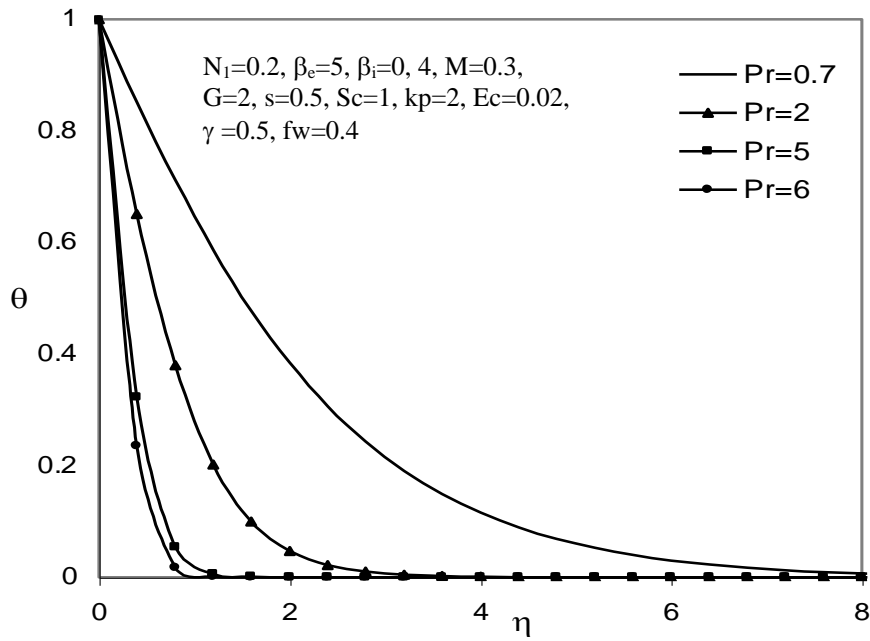


Fig.13 Temperature profiles for various values of Prandti number

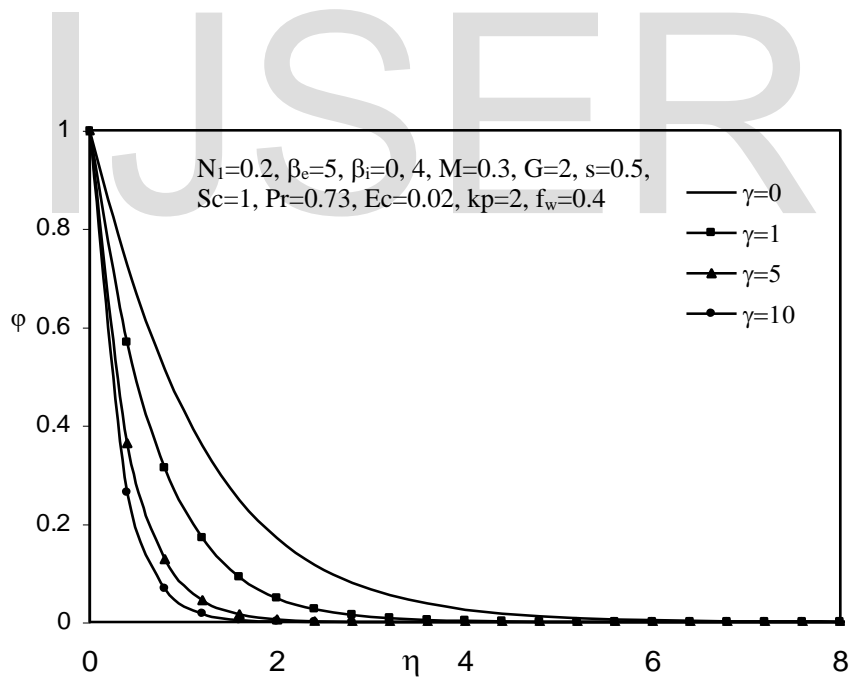


Fig.14 Concentration profiles for various values of chemical reaction parameter

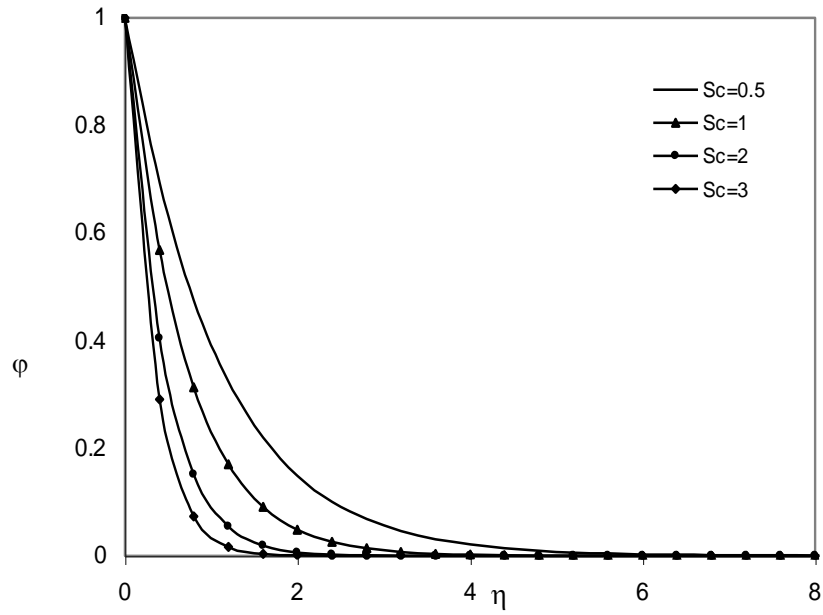


Fig.15 Concentration profiles for various values of Schmidt number

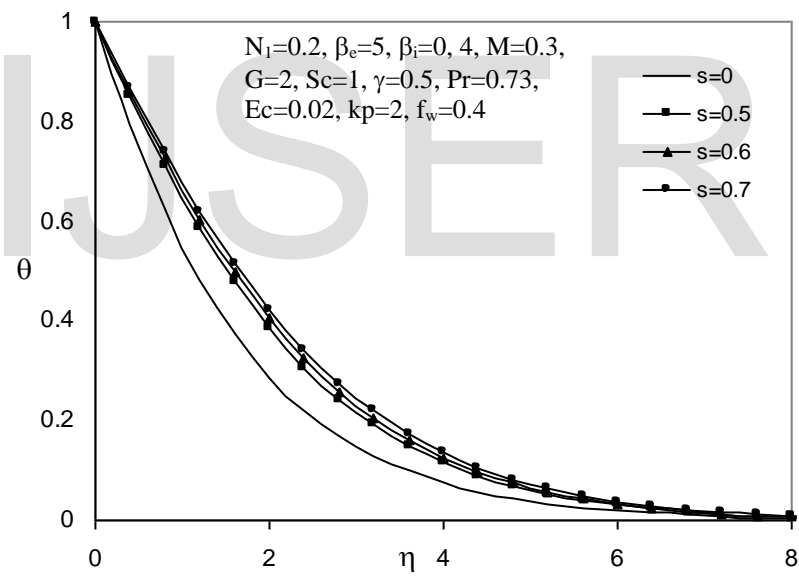


Fig. 16 Temperature profiles for various values of thermal conductivity parameter.

Table 1 (values of $-f''(0)$, $g'(0)$, $h'(0)$, $-\theta'(0)$, $-\phi'(0)$ for various values of coupling constant parameter N_1 at $k_p=2$, $\beta_e=5$, $\beta_i=0, 4$, $M=0.3$, $G=2$, $s=0.5$, $Sc=1$, $Pr=0.73$, $Ec=0.02$, $\gamma=0.5$, $f_w=0.4$)

N_1	$-f''(0)$	$g'(0)$	$h'(0)$	$-\theta'(0)$	$-\phi'(0)$
0	1.34769	0.0192493	0.276584	0.381572	0.895694
0.1	1.34336	0.0191923	0.276994	0.380651	0.895609
0.2	1.33875	0.0191337	0.277413	0.379703	0.895521
0.3	1.33412	0.0190735	0.277841	0.378727	0.895429

Table 2 (values $-f''(0)$, $g'(0)$, $h'(0)$, $-\theta'(0)$, $-\phi'(0)$ for various values of porous medium parameter k_p at $N_1=0.2$, $\beta_e=5$, $\beta_i=0, 4$, $M=0.3$, $G=2$, $s=0.5$, $Sc=1$, $Pr=0.73$, $Ec=0.02$, $\gamma=0.5$, $f_w=0.4$)

k_p	$-f''(0)$	$g'(0)$	$h'(0)$	$-\theta'(0)$	$-\phi'(0)$
0.5	1.77308	0.0113448	0.307905	0.326878	0.875106
1	1.50612	0.0154241	0.290595	0.357338	0.887022
1.5	1.39792	0.0176764	0.282307	0.371489	0.892415
2	1.33875	0.0191337	0.277413	0.379703	0.895521

Table 3 (values $-f''(0)$, $g'(0)$, $h'(0)$, $-\theta'(0)$, $-\phi'(0)$ for various values of Hall parameter β_e at $N_1=0.2$, $k_p=2$, $\beta_i=0, 4$, $M=0.3$, $G=2$, $s=0.5$, $Sc=1$, $Pr=0.73$, $Ec=0.02$, $\gamma=0.5$, $f_w=0.4$)

β_e	$-f''(0)$	$g'(0)$	$h'(0)$	$-\theta'(0)$	$-\phi'(0)$
5	1.33875	0.0191337	0.277413	0.379703	0.895521
7	1.34282	0.0157169	0.277764	0.379117	0.895301
10	1.34552	0.0119545	0.277997	0.378727	0.895155
15	1.34716	0.0083558	0.278139	0.378489	0.895066

Table 4 (values $-f''(0)$, $g'(0)$, $h'(0)$, $-\theta'(0)$, $-\phi'(0)$ for various values of ion-slip parameter β_i at $N_1=0.2$, $k_p=2$, $\beta_e=5$, $M=0.3$, $G=2$, $s=0.5$, $Sc=1$, $Pr=0.73$, $Ec=0.02$, $\gamma=0.5$, $f_w=0.4$)

β_i	$-f''(0)$	$g'(0)$	$h'(0)$	$-\theta'(0)$	$-\phi'(0)$
0	1.34407	0.0250583	0.277815	0.378975	0.895242
0.2	1.34079	0.0224459	0.277580	0.379426	0.895414
0.4	1.33875	0.0191337	0.277413	0.379703	0.895521
0.6	1.33779	0.0158620	0.277337	0.379829	0.895570

Table 5 (values $-f''(0)$, $g'(0)$, $h'(0)$, $-\theta'(0)$, $-\phi'(0)$ for various values of microrotation parameter G at $N_1=0.2$, $k_p=2$, $\beta_e=5$, $M=0.3$, $\beta_i=0.4$, $s=0.5$, $Sc=1$, $Pr=0.73$, $Ec=0.02$, $\gamma=0.5$, $f_w=0.4$)

G	$-f''(0)$	$g'(0)$	$h'(0)$	$-\theta'(0)$	$-\phi'(0)$
1	1.33535	0.0190858	0.457630	0.378805	0.895335
2	1.33875	0.0191337	0.277413	0.379703	0.895521
4	1.34166	0.0191748	0.161035	0.380440	0.895639
6	1.34305	0.0191944	0.115233	0.380774	0.895681
8	1.34389	0.0192061	0.090299	0.380965	0.895700

Table 6 (values $-f''(0)$, $g'(0)$, $h'(0)$, $-\theta'(0)$, $-\phi'(0)$ for various values of magnetic parameter M at $N_1=0.2$, $k_p=2$, $\beta_e=5$, $G=2$, $\beta_i=0.4$, $s=0.5$, $Sc=1$, $Pr=0.73$, $Ec=0.02$, $\gamma=0.5$, $f_w=0.4$)

M	$-f''(0)$	$g'(0)$	$h'(0)$	$-\theta'(0)$	$-\phi'(0)$
0	1.34860	3.98484×10^{-14}	0.278263	0.378281	0.894989
0.1	1.34537	0.0063867	0.277989	0.378739	0.895161
0.2	1.34209	0.0127641	0.277706	0.379213	0.895339
0.3	1.33875	0.0191337	0.277413	0.379703	0.895521

Table 7 (values $-f''(0)$, $g'(0)$, $h'(0)$, $-\theta'(0)$, $-\phi'(0)$ for various values of mass transfer parameter f_w at $N_1=0.2$, $k_p=2$, $\beta_e=5$, $G=2$, $\beta_i=0.4$, $s=0.5$, $Sc=1$, $Pr=0.73$, $Ec=0.02$, $\gamma=0.5$, $M=0.3$)

f_w	$-f''(0)$	$g'(0)$	$h'(0)$	$-\theta'(0)$	$-\phi'(0)$
-0.4	0.97483	0.0200189	0.239762	0.151385	0.696018
-0.2	1.05470	0.0201029	0.249229	0.198584	0.742048
0	1.14193	0.0199838	0.258730	0.253031	0.790648
0.2	1.23663	0.0196576	0.268162	0.313750	0.841811
0.4	1.33875	0.0191337	0.277413	0.379703	0.895521

Table 8 (values of $-\theta'(0)$ for various values of thermal conductivity parameter s , Prandti number Pr , and Eckert number Ec at $N_1=0.2$, $k_p=2$, $\beta_e=5$, $G=2$, $\beta_i=0.4$, $Sc=1$, $\gamma=0.5$, $M=0.3$, $f_w=0.4$)

Ec	s	$Pr = 2$	$Pr = 3$	$Pr = 4$	$Pr = 5$
0	0	0.792822	1.065320	1.31697	1.55740
	0.2	0.682191	0.915902	1.13323	1.34423
	0.4	0.601198	0.804398	0.991749	1.17398
	0.6	0.539829	0.720029	0.883369	1.04064
0.2	0	0.607666	0.794912	0.962988	1.121140
	0.2	0.524505	0.683326	0.825003	0.959049
	0.4	0.464744	0.602872	0.723691	0.836923
	0.6	0.419777	0.543175	0.648531	0.745294
0.4	0	0.422509	0.524505	0.609003	0.684871
	0.2	0.368046	0.453657	0.522169	0.582559
	0.4	0.329761	0.404894	0.462440	0.511259
	0.6	0.301121	0.369658	0.420155	0.491012

Table 9 (values of $-\phi'(0)$ for various values of chemical reaction parameter γ , Schmidt number Sc , and Hall parameter β_e at $N_1=0.2$, $k_p=2$, $s = 0.5$, $G = 2$, $\beta_i=0.4$, $Ec=0.02$, $Pr = 0.73$, $M=0.3$, $f_w=0.4$)

β_e	γ	$Sc = 0.1$	$Sc = 0.5$	$Sc = 1$	$Sc = 1.5$
5	0.2	0.205892	0.562507	0.93407	1.27107
	0.4	0.252266	0.667916	1.06529	1.41518
	0.6	0.292002	0.754226	1.17540	1.53747
	0.8	0.327057	0.828905	1.27152	1.64447
	1	0.358639	0.895521	1.35743	1.73995
7	0.2	0.205817	0.562192	0.93357	1.27043
	0.4	0.252199	0.667665	1.06488	1.41465
	0.6	0.291941	0.754011	1.17505	1.53702
	0.8	0.327000	0.828714	1.27121	1.64406
	1	0.358586	0.895347	1.35715	1.73957
15	0.2	0.205728	0.561817	0.93297	1.26968
	0.4	0.252120	0.667366	1.06440	1.41402
	0.6	0.291868	0.753755	1.17464	1.53647
	0.8	0.326933	0.828486	1.27084	1.64357
	1	0.358522	0.895139	1.35682	1.73912

Table 10 (values of $\varphi(\eta)$ for various values of Hall parameter β_e at $N_1=0.2$, $k_p=2$, $f_w=0.4$, $G=2$, $\beta_i=0.4$, $s=0.5$, $Sc=1$, $Pr=0.73$, $Ec=0.02$, $\gamma=0.5$, $M=0.3$)

η	$\beta_e=5$	$\beta_e=7$	$\beta_e=10$	$\beta_e=15$
	$\varphi(\eta)$	$\varphi(\eta)$	$\varphi(\eta)$	$\varphi(\eta)$
0	1	1	1	1
0.4	0.69351	0.693571	0.693614	0.693645
0.8	0.475613	0.475718	0.47579	0.475842
1.2	0.324047	0.324172	0.324258	0.324321
1.6	0.219949	0.220076	0.220164	0.220228
2	0.148974	0.149091	0.149173	0.149231
2.4	0.100782	0.100885	0.100955	0.101006
2.8	0.068137	0.068222	0.068281	0.068323
3.2	0.046051	0.046119	0.046166	0.0462
3.6	0.031118	0.031172	0.031209	0.031236
4	0.021026	0.021067	0.021096	0.021116
4.4	0.014205	0.014237	0.014259	0.014274
4.8	0.009597	0.00962	0.009636	0.009648
5.2	0.006482	0.0065	0.006512	0.00652

Table 11 (values of $\varphi(\eta)$ for various values of coupling constant parameter N_1 at $\beta_e=5$, $k_p=2$, $f_w=0.4$, $G=2$, $\beta_i=0.4$, $s=0.5$, $Sc=1$, $Pr=0.73$, $Ec=0.02$, $\gamma=0.5$, $M=0.3$)

η	$N_1=0$	$N_1=0.1$	$N_1=0.2$	$N_1=0.3$
	$\varphi(\eta)$	$\varphi(\eta)$	$\varphi(\eta)$	$\varphi(\eta)$
0	1	1	1	1
0.4	0.693426	0.693467	0.69351	0.693554
0.8	0.475428	0.47552	0.475613	0.47571
1.2	0.323763	0.323903	0.324047	0.324194
1.6	0.219593	0.219769	0.219949	0.220133
2	0.148585	0.148777	0.148974	0.149175
2.4	0.100396	0.100587	0.100782	0.100982
2.8	0.067779	0.067956	0.068137	0.068322
3.2	0.045736	0.045892	0.046051	0.046214
3.6	0.030853	0.030984	0.031118	0.031256
4	0.020808	0.020916	0.021026	0.021138
4.4	0.014032	0.014118	0.014205	0.014295
4.8	0.009461	0.009528	0.009597	0.009667
5.2	0.006378	0.006429	0.006482	0.006536

Table 12 (values of $\varphi(\eta)$ for various values of ion-slip parameter β_i at $N_1=0.2$, $k_p=2$, $f_w=0.4$, $G=2$, $\beta_e=5$, $s=0.5$, $Sc=1$, $Pr=0.73$, $Ec=0.02$, $\gamma=0.5$, $M=0.3$)

$\sigma\zeta$	$\beta_i=0$	$\beta_i=0.2$	$\beta_i=0.5$	$\beta_i=1$
	$\varphi(\eta)$	$\varphi(\eta)$	$\varphi(\eta)$	$\varphi(\eta)$
0	1	1	1	1
0.4	0.693608	0.693547	0.693499	0.693493
0.8	0.475779	0.475677	0.475595	0.475586
1.2	0.324244	0.324122	0.324025	0.324014
1.6	0.220149	0.220025	0.219927	0.219916
2	0.149158	0.149044	0.148953	0.148944
2.4	0.100942	0.100843	0.100765	0.100757
2.8	0.068269	0.068187	0.068123	0.068116
3.2	0.046157	0.046091	0.046039	0.046034
3.6	0.031201	0.03115	0.031109	0.031105
4	0.02109	0.02105	0.021019	0.021016
4.4	0.014254	0.014224	0.0142	0.014198
4.8	0.009633	0.00961	0.009593	0.009591
5.2	0.006509	0.006492	0.006479	0.006478

5. The discussion of the results

It is clear that increase the value of the dimensionless porous parameter moves the location of the maximum value of the microrotation away from the surface as shown in (Fig. 1). It can be seen that the velocity and the angular velocity increase with the increases of the dimensionless porous parameter as shown in (Fig. 2), (Fig.3). Temperature and concentration decrease with increases in the dimensionless porous parameter as shown in (Fig. 4), (Fig.5). (Fig. 6) indicates the effect of ion-slip parameter. With increases in ion-slip parameter, angular velocity decreases. It can be seen that the velocity, the angular velocity, the temperature, and the concentration increase with injection and decrease with increases in suction as shown in Fig. (7-11). (Fig.8) indicates the effect of mass transfer parameter on a microrotation. The micro rotation reaches a maximum and then decay to zero. Increasing values of the injection parameter move the location of the maximum value of the microrotation away from the surface. The microrotation decreases with the increase in suction. The temperature increases with increase in Eckert number, thermal conductivity parameter but it decreases with increases in Prandtl number as shown in (Fig.12), (Fig. 13), and (Fig. 16). The concentration decreases with increase in chemical reaction parameter, Schmidt number as shown in (Fig. 14), (Fig. 15).

The effect of coupling constant parameter N_1 on the values of $-f''(0)$, $g'(0)$, $h'(0)$, $-\theta'(0)$, $-\varphi'(0)$ is indicated in (table 1). It can be seen that values of $-f''(0)$, $g'(0)$, $-\theta'(0)$ and $-\varphi'(0)$ decrease but, values of $h'(0)$ increase, as the coupling constant parameter increase. The effect of porous medium parameter k_p on the values of $-f''(0)$, $g'(0)$, $h'(0)$, $-\theta'(0)$, $-\varphi'(0)$ appears in (table 2). It can be seen that values of $-f''(0)$, $h'(0)$ decrease but values of $g'(0)$, $-\theta'(0)$, $-\varphi'(0)$ increase as the porous medium parameter increases. The effect of Hall parameter β_e on the values of $-f''(0)$, $g'(0)$, $h'(0)$, $-\theta'(0)$, $-\varphi'(0)$ showed in (table 3). It observed that values of $-f''(0)$, $h'(0)$ increase, but values of $g'(0)$, $-\theta'(0)$, $-\varphi'(0)$ decrease as the Hall parameter increases. The effect of ion-slip parameter β_i on the values of $-f''(0)$, $g'(0)$, $h'(0)$, $-\theta'(0)$, $-\varphi'(0)$ appears in (table 4). Values of $-f''(0)$, $g'(0)$, $h'(0)$ decrease, but values $-\theta'(0)$, $-\varphi'(0)$ increase as the ion-slip parameter increases. (Table 5) indicates the effect of microrotation parameter G on the values of $-f''(0)$, $g'(0)$, $h'(0)$, $-\theta'(0)$, $-\varphi'(0)$. It can be seen that values of $-f''(0)$, $g'(0)$, $-\theta'(0)$, $-\varphi'(0)$. increase, but values of $h'(0)$ decrease as the microrotation parameter increases. The effect of magnetic parameter M on the values of $-f''(0)$, $g'(0)$, $h'(0)$, $-\theta'(0)$, $-\varphi'(0)$ appears in (Table 6). It is clear that values of $-f''(0)$, $h'(0)$ decrease, but values of $g'(0)$, $-\theta'(0)$, $-\varphi'(0)$ increase, as the magnetic parameter increases. (Table 7) indicates the effect of mass transfer parameter f_w on the values of $-f''(0)$, $g'(0)$, $h'(0)$, $-\theta'(0)$, $-\varphi'(0)$. It can be seen that increase injection decrease values of $-f''(0)$, $g'(0)$, $h'(0)$, $-\theta'(0)$, $-\varphi'(0)$. Also it is clear that suction has an opposite effect. (Table 8) displays the effect of Eckert number Ec , the thermal conductivity parameter s , and Prandtl number Pr on $-\theta'(0)$. It is note that $-\theta'(0)$ decreases with the Eckert number. It decreases with the thermal conductivity parameter and increases with the Prandtl number. (Table 9) displays the effect of the Hall parameter β_e , the chemical reaction parameter γ , and Schmidt number Sc on $-\varphi'(0)$. It is note that $-\varphi'(0)$ decreases with the Hall parameter. It increases with the chemical reaction parameter and increases with the Schmidt number. The effect of Hall parameter β_e on the values of $\varphi(\eta)$ appears in (Table 10). It observed that value of $\varphi(\eta)$ increase, as the Hall parameter increases. (Table 11) indicates the effect of coupling constant parameter N_1 on the values of $\varphi(\eta)$. It observed that value of $\varphi(\eta)$ increase, as the coupling constant parameter increases. The effect of ion-slip parameter β_i on the values of $\varphi(\eta)$ appears in (Table 12). Values of $\varphi(\eta)$ decrease, as the ion-slip parameter increases.

6. Conclusions

In this paper, we have presented a study of an incompressible, magneto-micropolar fluid flowing through a porous medium past a horizontal stretching sheet under the effects of both Hall and ion-slip currents, chemical reaction, and variable thermal conductivity. A similarity transformation was employed to change the governing partial differential equations into ordinary differential equations. These equations were solved numerically by using finite difference method. Velocity, temperature, and concentration fields are presented for various values of the parameters of the problem, e.g., magnetic, Hall, ion-slip, chemical reaction, porous medium, thermal conductivity, mass transfer parameters. The numerical results indicate that, the concentration profiles decrease as the ion-slip, porous medium and chemical reaction parameters increase. It increases as the Hall, coupling constant parameters increase. It also increases with injection and suction has an opposite effect. We notice that, the effect of porous medium parameter becomes smaller as its values increase. This result can be achieved when the holes of the porous medium are very large so that the resistance of the medium may be neglected.

IJSER

References

- [1] Eringen, A. C., Theory of micropolar fluid, *Journal of Mathematics and Mechanics*, 16 (1966) 1-18.
- [2] Eringen, A. C., Theory of thermo-micro fluids, *Journal of mathematical analysis and applications*, 38(1972) 480 – 496.
- [3] Gorla, R. S., Takhar, H. S., and Slaouti, A., Magneto hydrodynamic free convection boundary layer flow of a thermomicro polar fluid over a vertical plate, *International Journal of Engineering Science*, 36 (1998) 315 – 327.
- [4] Malashetty, M. S., Cheng, P., and Chao, B. H., Convective instability in a horizontal porous layer saturated with a chemically reacting fluid, *international journal of heat and mass transfer*, 37 (1994) 2901 – 2908.
- [5] El Tawil, M. A., and Hassanien, I, A., The computer simulation study of the stochastic chemical reaction in a laminar boundary layer flow over a stretching surface, *Journal of inst. Math. & Comp. Sci.*, 6 (1995) 105 – 120.
- [6] El-Adawi, M.K., Elshehawey, E. F., Shalaby, A.S, The Stability of Nature convection in an inclined fluid layer in the presence of temperature gradient and A.C electric field. *Canadian J of phy*, 75(1997)299-311
- [7] Kumar, H.Mixed convective magneto hydrodynamic(MHD) flow of a micro polar fluid with Ohmic heating radiation and viscous dissipation over a chemically reacting porous plate subjected to a constant heat flux and concentration gradient,*J.Serb.Chem.Soc.*,78 (2013) 1-17.
- [8] Singh, K., Kumar, M. The effect of chemical reaction and double stratification on mhd free convection in a micro polar fluid with heat generation and ohmic heating, *Journal of Mechanical and Industrial Engineering*, 9 (2015) 279-288.
- [9] Chamkha, A. J., MHD free convection from a vertical plate embedded in a thermally porous medium with Hall effects, *Applied Mathematical Model*, 21(1997) 603.
- [10] Sedeek, M. A., The effects of Hall and ion-slip currents on a magneto-micropolar fluid and the heat transfer over a non-isothermal stretching sheet with suction and blowing, *Proc. R. Soc.*, 457 (2001) 1.
- [11] Aboeldahab, E. M., and Elbarbary, E. M. E., The Hall current effect on MHD free convection flow past a semi-infinite vertical plate with mass transfer, *International Journal of Engineering Science*, 39 (2001) 1641.
- [12] Takhar, H. S., Chamkha, A. J., and Nath, G., MHD flow over a moving plate in a rotating fluid with magnetic field, Hall currents, and free stream velocity, *International Journal of Engineering Science*, 40 (2002) 1511 – 1527
- [13] Elshehawey, E. F., Eldabe, N. T., Elbarbary, E. M. E., and Elgazery, N. S., Chebyshev finite-difference method for the effects of Hall and ion-slip currents on magneto-hydrodynamic flow with variable thermal conductivity, *Can. J. Phy.*, 82 (2004) 1 – 15.
- [14] Takhar, H. S., Chamkha, A. J., and Nath, G., Flow and Mass Transfer on a stretching sheet with a magnetic field and chemically reactive species, *International Journal of Engineering Science*, 38 (2000) 1303 – 1314.